



## Actuator and generator based on moisture-responsive PEDOT: PSS/PVDF composite film



Gong Wang<sup>a</sup>, Hong Xia<sup>a,\*</sup>, Xiang-Chao Sun<sup>a</sup>, Chao Lv<sup>a</sup>, Shun-Xin Li<sup>a</sup>, Bing Han<sup>a</sup>, Qi Guo<sup>a</sup>, Qing Shi<sup>a</sup>, Ying-Shuai Wang<sup>a</sup>, Hong-Bo Sun<sup>a,b</sup>

<sup>a</sup> State Key Laboratory on Integrated Optoelectronics, College of Electronic Science and Engineering, Jilin University, 2699 Qianjin Street, Changchun 130012, China

<sup>b</sup> College of Physics, Jilin University, 119 Jiefang Road, Changchun 130023, China

### ARTICLE INFO

#### Article history:

Received 28 February 2017

Received in revised form 15 June 2017

Accepted 15 August 2017

Available online 23 August 2017

#### Keywords:

PEDOT: PSS/PVDF

Actuator

Generator

Moisture-responsive

### ABSTRACT

Energy conversion via utilizing small changes in the environment is emerging as an attractive way to mitigate energy crisis. Although some pioneering works have already shown the advantages of these energy conversion devices, challenges remain, including complex preparation process, excessive energy loss and difficult application of alternating current output. Here, we report a facile, cost-effective method for preparing a moisture-responsive composite film combined both PEDOT: PSS and piezoelectric polymer PVDF by means of spin coating and thermal evaporation. The composite film possesses good bidirectional bending performance, and the bending angles in both directions can reach 191° and 225° respectively. The generator based on this composite film is capable of producing a stable direct current voltage output up to 150 mV and charging the capacitor without any energy-consuming rectifier circuit. Our approach provides a new, simple, promising strategy for low-frequency small-signal energy collection and utilization.

© 2017 Elsevier B.V. All rights reserved.

### 1. Introduction

As environment challenges, energy shortage and other issues become more and more serious, the development of renewable green energy is particularly important. The energy sources, such as solar energy [1], hydropower [2], wind power [3], biomass energy [4], tidal energy [5] and geothermal energy [6], have attracted people's extensive research and attention. To acquire these green renewable energy sources, large-scale sophisticated equipment is needed to preform massively energy conversion. However, it is worth noting that there are many small changes such as heat [7], humidity [8], pressure [9] and mechanical motion [10,11], which can participate in the energy conversion. These scattered, small changes can produce tiny energy through certain energy conversion devices [12,13]. These tiny energies seem to be useless and insignificant, but they can also provide energy for some small self-powered systems when being accumulated. As a typical example of the tiny energy conversion method, nanogenerators have been developed rapidly in recent years. Nanogenerator possesses many advantages, such as flexibility, wearable [14], high output voltage etc. [15], but with complicated fabrication process, requirement of

a management circuit module and small output current limit its application.

The development of smart actuators whose mechanical motion can be controlled by external stimuli—such as light [16], humidity [17,18], pH value [19], temperature [20], and chemicals [21]—has recently received enormous research interests. To achieve such stimuli-responsive devices, the design and control of materials play an important role. It is worth noting that the macroscopic movement of intelligent devices is inseparable from the interaction of molecules [22]. The effects that occur in the microscopic level are usually similar to those in the macroscopic system [23]. In addition, there are some different effects on nanoscales also have an important impact on the dynamic properties of the materials. [23,24]. In nature, many organisms with double-layered structure will contract or expand differently under the stimulation of the external environment (e.g. pinecone) [25,26], which inspired us to use a double-layered structure in the fabrication of actuators to achieve anisotropic motion under external stimulus [27–29]. One layer of the double-layered actuator is a moisture-sensitive active layer, whereas the other one is an inert layer that is not sensitive to the moisture. When the external humidity change, the moisture-sensitive layer expands or shrinks, while the volume of the inert layer barely changes. Therefore, the volume difference of the two layers is converted into a bending motion. In this work, the active layer of the double-layered actuator is conductive polymer

\* Corresponding author.

E-mail address: [hxia@jlu.edu.cn](mailto:hxia@jlu.edu.cn) (H. Xia).

poly(3,4-ethylenedioxythiophene): polystyrene sulfonate (PEDOT: PSS) and the inert layer is the piezoelectric material poly(vinylidene fluoride) (PVDF). The PEDOT: PSS as the active layer has exceptional moisture sensitivity and excellent mechanical properties. It also shows a good conductivity property which provides a wide range of applications in electrical devices. The PVDF as the inert layer is a commercial piezoelectric material with good chemical stability, plasticity and flexibility. It can convert mechanical energy into electrical energy and enables the actuators to be used for generating electricity.

The solution for gathering energy using stimuli-responsive actuators of single- or double-layered has been designed to transform mechanical energy into electrical energy [30–32]. The actuator is usually connected with the piezoelectric device which receives the mechanical motion that the actuator generates under the external stimulus. The deformation or movement on the piezoelectric device is converted into electric signals. However, there is major energy loss in the transmission process, and the output voltage produced is the alternating current (AC) signal. In this work, a methodology, which directly introduces the piezoelectric materials into the double-layered actuator, is proposed for the first time. It allows the generation of the electrical energy directly from the movement of the actuator, also eliminates the energy loss caused by the movement of the piezoelectric device driven by the actuator. The PEDOT: PSS was fabricated on the smooth PVDF film as a composite film, resulting in a close contact without any gap. The composite film is the double-layered actuator that has been mentioned. Containing water weight change in PEDOT: PSS during single absorption or desorption process can lead to the PVDF film deformation with single direction, which generates a stable direct current (DC) signal whose maximum value can up to 150 mV. The DC output does not require rectifier circuit and can be charged directly for the capacitor, which makes it a promising technique. Eventually, a circuit has been designed to solve the problem that the low-frequency small-signal DC output is difficult to be applied, which provides a new method for the collection and the utilization of low-frequency small-signal energy, and a new strategy for dealing with energy problems in the future.

## 2. Experiments

### 2.1. Fabrication of PEDOT:PSS/PVDF actuators and generator

A commercially available PVDF film (20  $\mu\text{m}$  thick, Jinzhou KEXIN Electronic Material Co., Ltd) having aluminum electrodes deposited on both sides was cut into a rectangle of 3 cm in length and 2 cm in width, and was fixed on a coverslip with a Kapton tape. The subsequent air plasma treatment (YZD08-2C Plasma Cleaner) was applied for 60 s at a power of  $P=25\text{ W}$ . A commercially available PEDOT: PSS aqueous dispersion (Clevios pH 1000, 1:2.5 PEDOT: PSS ratio; Heraeus Clevios GmbH) was deposited by spin coating at a rate of  $s=2000\text{ rpm}$  for 60 s onto the plasma-treated PVDF surface. After spin-coating, the sample was heated on a  $55\text{ }^\circ\text{C}$  hot stage for 5 min, and then subjected to air plasma treatment for 10 s at a power of  $P=25\text{ W}$ . The next layer of PEDOT: PSS was then spin-coated and the 16 layers of PEDOT: PSS were spin-coated as described above. After the final spin-coating, the sample was heated on a  $55\text{ }^\circ\text{C}$  hot stage for 1 h.

### 2.2. Fabrication of biomimetic dragonfly and three-layer-structure of flower

First, a commercially available PVDF film (10  $\mu\text{m}$  thick, Jinzhou KEXIN Electronic Material Co., Ltd) was pretreated according to the procedure described above for the fabrication of the PEDOT:

PSS/PVDF actuator. Second, the samples were cut and patterned using a direct write  $\text{CO}_2$  laser (JW6090, JWJG. Shandong) with tunable laser power (10% of the maximum) and scanning speed (80% of the maximum) and then a dragonfly (18 mm  $\times$  16 mm) and three four-petal flowers of different sizes (10 mm  $\times$  10 mm, 16 mm  $\times$  16 mm, 22 mm  $\times$  22 mm) could be obtained.

The 10 ml syringe needle was used to penetrate through the center of the three four-petal flowers, thereby assembling into a three-layer-structure of flower.

### 2.3. Characterization and measurement

SEM images were taken with a JEOL JSM-7500 field-emission scanning electron microscope (FE-SEM). The static water droplet contact angles (CAs) were measured using a Contact Angle Meter SL200 B (Solon Tech. Shanghai). Saturated aqueous solution was used to control the humidity environment in a closed glass vessel ( $P=101.3\text{ kPa}$ ,  $T=20\pm 0.5\text{ }^\circ\text{C}$ ), and seven relative humidity ranges of 23%, 33%, 44%, 57%, 75%, 86%, and 97% were generated using seven saturated aqueous solutions of  $\text{CH}_3\text{COOK}$ ,  $\text{MgCl}_2$ ,  $\text{K}_2\text{CO}_3$ ,  $\text{NaBr}$ ,  $\text{NaCl}$ ,  $\text{KCl}$ , and  $\text{K}_2\text{SO}_4$ , respectively. All of the measurements were conducted in air at room temperature ( $20\pm 0.5\text{ }^\circ\text{C}$ ). Current–voltage curves of the PEDOT: PSS layer and PVDF layer were measured with a Keithley 2400 programmable voltage-current characterization system.

## 3. Results and discussion

Fig. 1a shows the schematic illustration of the fabrication process for a PEDOT: PSS/PVDF double-layered actuator. The PVDF film deposited with aluminum electrode was fixed on the surface of the coverslip with Kapton tape, and then a surface plasma treatment was applied, which increased the hydrophilic groups of the film surface. Subsequently, PEDOT: PSS was spin-coated on PVDF film surface. In the experiment, PEDOT: PSS that was spin-coated on the PVDF film which was applied surface plasma treatment could evenly cover the entire PVDF film surface, whereas none of the PEDOT: PSS could remain on the PVDF film if no surface plasma treatment was applied. The PVDF film was then heated on a hot stage at  $55\text{ }^\circ\text{C}$  for 5 min to evaporate the water in the PEDOT: PSS. If the temperature of the hot stage was higher, thermal deformation would happen on the PVDF film which causes wrinkle, which was unfavorable for spin coating on the next layer. The procedure mentioned above was repeated, a total of 16 layers of PEDOT: PSS were spin-coated on the PVDF film. The PEDOT: PSS layer of the double-layered actuator exhibited a navy blue color with a metallic luster (Fig. 1b), and the PVDF layer exhibited a silvery white color with a metallic luster due to the deposition of an aluminum electrode on the surface (Fig. 1c). We measured the static water droplet contact angle (CA) on the two layers' surfaces of the double-layered actuator. As shown in Fig. 1b and c, the contact angle of the PEDOT: PSS layer is ca.  $81.76^\circ$  and the contact angle of the PVDF layer is ca.  $123.85^\circ$ . The values of CA indicate that the PEDOT: PSS layer is hydrophilic and the PVDF layer is hydrophobic, which proves that there is a large difference in the surface wettability of the double-layered actuator.

Fig. 1d is a scanning electron microscope (SEM) image of the double-layered actuator cross-section. It can be seen that the thickness of active layer PEDOT: PSS is  $1.2\pm 0.2\text{ }\mu\text{m}$ , and the inert layer PVDF is  $22\pm 1\text{ }\mu\text{m}$ , which is approximately 20 times of the active layer. Although the active layer is very thin compared to the inert layer, for the reason that the PEDOT: PSS has a good mechanical property, the flexible PVDF can be constrained, which results in a significant bending effect of the double-layered actuator when a slight contraction or expansion happens on the PEDOT: PSS layer

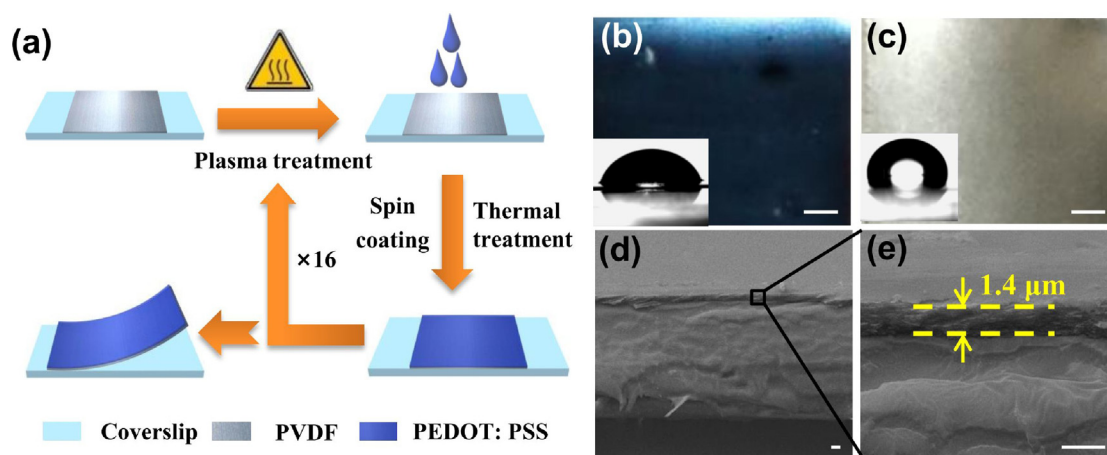


**Fig. 1.** (a) Schematic illustration of the fabrication process of the PEDOT: PSS/PVDF double-layered actuator. (b) and (c) Photographs of the PEDOT: PSS/PVDF double-layered actuator viewed from the PEDOT: PSS side (b) and the PVDF side (c), respectively (scale bar represents 1 mm). The insets show water droplet contact angles of both sides. (d) and (e) SEM images of a cross section of the PEDOT: PSS/PVDF double-layered actuator (scale bar represents 2  $\mu\text{m}$ ).

due to environmental stimuli. In addition, the thin active layer increases in the rate of moisture adsorption and desorption, as a result of which, increases the actuation speed of the double-layered actuator. It can be seen from Fig. 1e that there is no gap between the PEDOT: PSS layer and the PVDF layer. The two layers are very close together, which explains why the two layers of the double-layered actuator will not be separated easily. Since the PEDOT: PSS layer in the fabrication is processed by multiple spin-coating, its multilayer structure can be seen in Fig. 1e. This stacked multilayer structure is able to reduce mechanical damage during actuation, which has been proved in other literatures [33].

The PEDOT: PSS/PVDF double-layered actuator has a lateral anisotropy property, thus it exhibits significant moisture-responsive bending properties. The mechanism of the PEDOT: PSS/PVDF double-layered actuator bidirectional bending is shown in Fig. 2a. When the moisture content in the environment is lower than that in the PEDOT: PSS film, the PEDOT: PSS film desorbs water and shrinks, and the double-layered actuator bends to the PEDOT: PSS side; when the moisture content in the environment is higher than that in the PEDOT: PSS film, the PEDOT: PSS film adsorbs water and swells, and the double-layered actuator bends to the PVDF side. In order to quantitatively study the actuating behavior of the double-layered actuator, the curvature degrees variation of the PEDOT: PSS/PVDF strip at relative humidity (RH) from 23% to 97% was measured [34], as shown in Fig. 2b. We specify that the curvature degree is negative when the PEDOT: PSS/PVDF strip is bent toward the PEDOT: PSS side and positive when bending toward the PVDF side. As the RH increased from 23% to 86%, the curvature degree changed from  $-191^\circ$  to  $225^\circ$ , in which the curvature degree was  $0^\circ$  at a RH of 57%. However, when the RH increased from 86% to 97%, the curvature degree decreased from  $225^\circ$  to  $212^\circ$ . The phenomenon can be explained by the fact that the moisture content is too high at RH = 97%. The PEDOT: PSS layer absorbs water excessively causing its mechanical property to be weak, so that the constrain ability to the PVDF layer weakens. Therefore, the curvature degree is smaller at RH = 97% than at RH = 86%. In order to study the response recovery performance of the double-layered actuator, the PEDOT: PSS/PVDF strip were switched between RH = 23% and RH = 86%, the curvature degree changing with time is shown in Fig. 2c. When the PEDOT: PSS/PVDF strip is moved from RH = 23% to RH = 86%, it will rapidly change bending from the side of PEDOT: PSS to the side of PVDF. The average response time for the change in the curvature degree of the PEDOT: PSS/PVDF strip is 10 s when the humidity is switched from RH = 23% to RH = 86%, and the average response time is 6 s when the humidity is switched from RH = 86% to

RH = 23%. Fig. 2c also demonstrates that the bending of the PEDOT: PSS/PVDF strip at different RHs is recyclable and repeatable.

The bending stability of the PEDOT: PSS/PVDF strip has been tested. The relation between the curvature degrees and the placement time of the PEDOT: PSS/PVDF strip is shown in Fig. 2d. When the strip was placed in the room for 100 days, the curvature angle was decreased by 4.8% compared to the initial value at RH = 23%, and was decreased by 9.2% compared to the initial value at RH = 86%. This result indicates that the PEDOT: PSS/PVDF strip could bend in both directions for more than 90% of the original performance within 100 days in lab environment ( $T = 20 \pm 0.5^\circ\text{C}$ ), which proves that PEDOT: PSS/PVDF strip has good stability and has broad application prospect. The current-voltage curves of the two different layers of the double-layered actuator have also been tested as shown in Fig. 2e. The PEDOT: PSS layer had good electrical conductivity, the resistance values of PEDOT: PSS layer before and after humidification were  $487.7\ \Omega$  and  $423.0\ \Omega$  respectively, indicating that the humidification process had a little improvement on the conductivity. The inset in Fig. 2e is the current-voltage curve for the PVDF layer, which is similar to the open-circuit test curve, indicating that the PVDF layer is insulated.

Based on the excellent moisture response performance of PEDOT: PSS/PVDF double-layered actuator and its bidirectional bending ability [35,36], a biomimetic dragonfly was fabricated. The fabricated PEDOT: PSS/PVDF composite film was carved into a dragonfly shape by a  $\text{CO}_2$  laser. The body of the dragonfly was stuck on one end of a capillary with double-sided adhesive. The other end of the capillary was fixed on the foam, which makes the dragonfly in a floating state. Fig. 3a shows the initial state of the dragonfly. Consistent with the previous conclusion, the dragonfly wings bend toward the PEDOT: PSS side under the humidity of lab environment at 30%. When applying water vapor, the ambient humidity around the wings was instantly shifted to a high value (RH > 80%). The change of the wings is shown in Fig. 3a–d. The maximum angle of the dragonfly wings bending to the PVDF side at high humidity is shown in Fig. 3d. When stopped the application of water vapor, the ambient humidity gradually decreased back to the original RH = 30%. The dragonfly wings recovered from bending to the PVDF side to the initial state, as shown in Fig. 3e–h. The process of the moisture absorption of the dragonfly wings bending to the PVDF side took 4.6 s; and the moisture desorption of the dragonfly wings bending to the PEDOT: PSS side took 6.3 s, which indicates that the moisture absorption rate was slightly faster than the desorption rate. The dynamic flapping process of dragonfly wings is shown in Movie S1. The dragonfly wings are able to achieve reversible

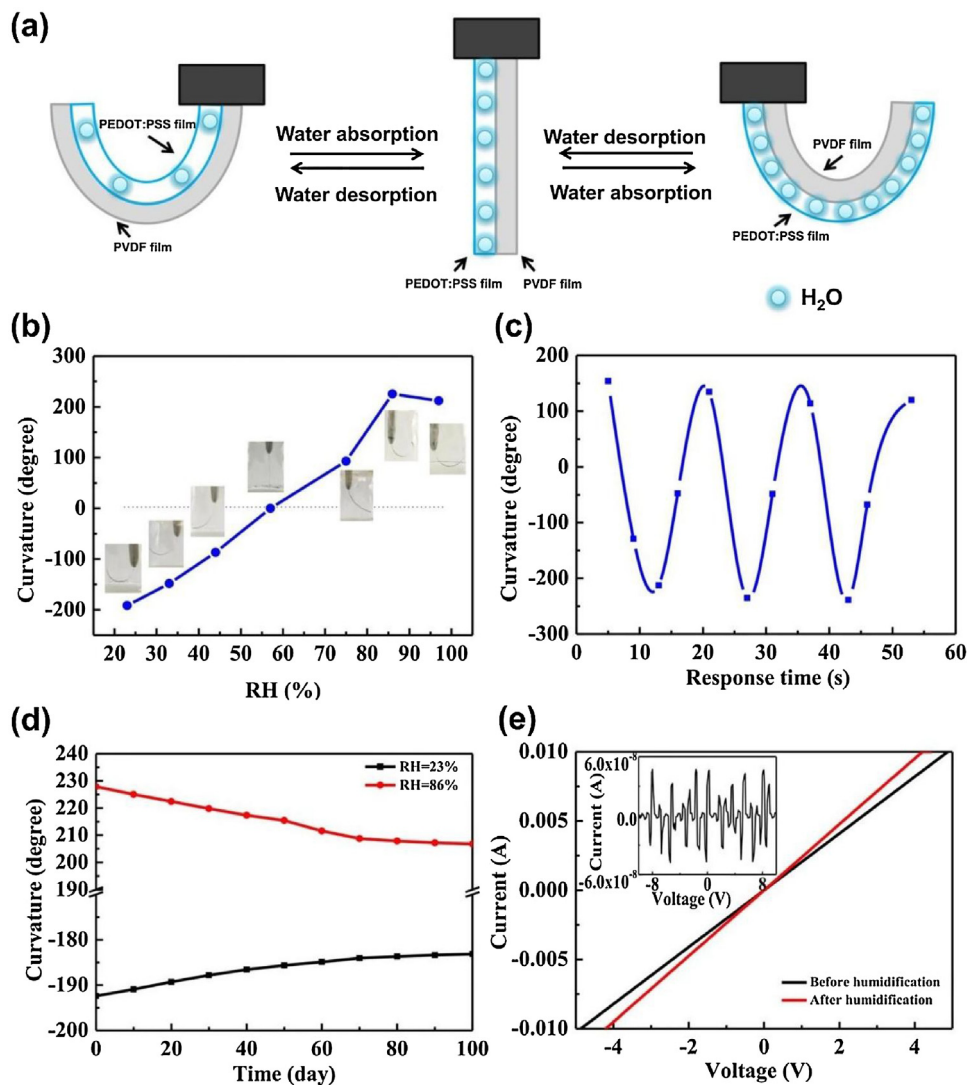


**Fig. 2.** (a) Schematic illustration of the bidirectional bending actuation mechanism of the PEDOT: PSS/PVDF double-layered actuator. (b) Dependence of the curvature of the PEDOT: PSS/PVDF strip on RH. (c) Responsive and recovery properties of the PEDOT: PSS/PVDF strip. RH was switched between 23% and 86% three times. (d) Dependence of the curvature of the PEDOT: PSS/PVDF strip on placement time. (e) Current-voltage ( $I$ - $V$ ) characteristics of the PEDOT: PSS layer, the inset is the  $I$ - $V$  characteristics of the PVDF layer.

bidirectional bending along with the ambient humidity changes, indicating that the PEDOT: PSS/PVDF double-layered actuator has a great potential in biomimetic applications.

In addition to moisture-controlled "biomimetic dragonflies", the moisture-sensitive PEDOT: PSS/PVDF composite film can also be used to produce other multi-stage intelligent devices. Fig. 3i-l shows another example: a three-layer-structure flower. PEDOT: PSS/PVDF composite films were carved into three different sized four-petal flowers using a CO<sub>2</sub> laser. They were strung together with a syringe needle to assemble a three-layer-structure flower. Fig. 3i-l illustrates the dehumidification process, which took 31.1 s that is far longer than the time took in the humidification process of 4.6 s. Fig. 3l is the final state. It is showed that the smallest and medium-sized four-petal flower did not change much during the dehumidification process, and the largest four-petal flower changed bending from the side of PVDF to the side of PEDOT: PSS (Movie S2). Three-layer-structure flower shows that, through the external constraints and the control of the size, different components of a same intelligent device in humidity controlled environment can conduct different actions. This means that PEDOT:

PSS/PVDF multi-stage intelligent devices have promising futures in sensing and other fields.

The PEDOT: PSS/PVDF double-layered actuator acts as a generator when connected to an external circuit, which exhibits a good ability to utilize ambient humidity changes to generate electricity. It is worth noting that unlike the AC signal generated by conventional energy conversion using PVDF [37], our PEDOT: PSS/PVDF double-layered generator is capable of generating a stable DC signal. Zhang et al. reported that a humidity-responsive actuator and a PVDF piezoelectric device was connected head-to-tail with silk thread [32]. Ma et al. presented an actuator which was attached to one side of a piezoelectric PVDF film without a complete contact [30]. In these researches, actuators and piezoelectric units were different individuals. The piezoelectric units deformed which was caused by its movement driven by the movement of the actuator. There was major energy loss throughout the movement transmitting process. Moreover, for the reason that the movement of the actuator was not in a single direction, it generated an AC signal. In our work, PEDOT: PSS was spin-coated on the smooth PVDF film as a composite film, resulting in a close contact without any gap. Containing water weight change in PEDOT: PSS during single

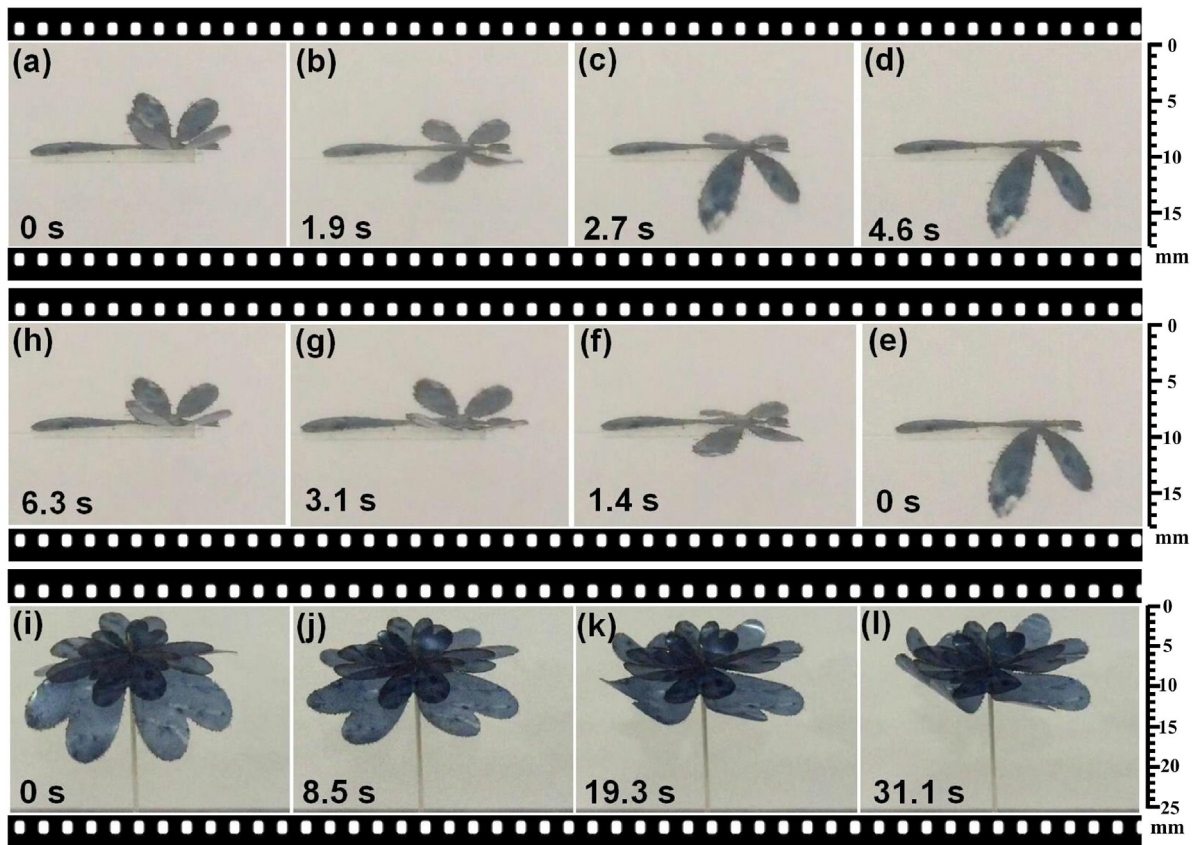


**Fig. 3.** (a)–(h) Biomimetic dragonflies with moisture response fabricated by PEDOT: PSS/PVDF composite film. (i)–(l) Three-layer-structure of flower assembled from three different sized four-petal flowers. The different components of the three-layer-structure of flower produce different responses under the same external stimuli.

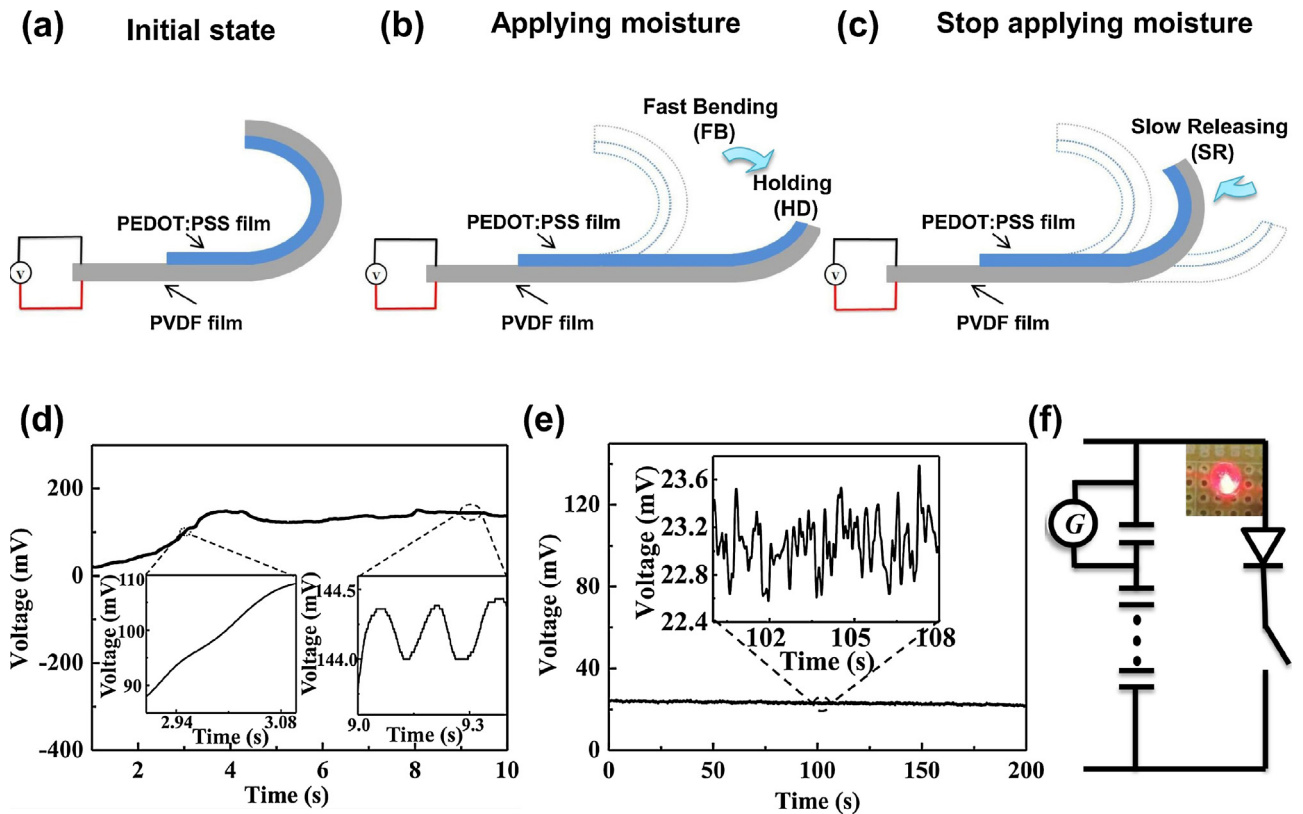


**Fig. 4.** (a)–(c) Schematic illustration of the PEDOT: PSS/PVDF double-layered generator produce a stable DC output voltage. (d) and (e) The output electrical signal generated by the generator during the humidification process (d) and dehumidification process (e), respectively. The inset is an enlarged view of the region of the curve. (f) The equivalent circuit diagram of the PEDOT: PSS/PVDF double-layered generator charges the capacitor to turn on the LED. The inset is the illuminated LED.

absorption or desorption process can lead to the PVDF film deformation with single direction, which generates a DC signal. Fig. 4a–c is a schematic of the PEDOT: PSS/PVDF double-layered generator that generates a DC signal. Fig. 4a shows PEDOT: PSS/PVDF double-layered generator without water vapor. The PEDOT: PSS-coated portion bent to the PEDOT: PSS side. The portion without the PEDOT: PSS layer was fixed on the glass slide, and from whose upper and lower sides of the PVDF led a wire respectively and connected to the oscilloscope. When water vapor was applied to the PEDOT: PSS/PVDF double-layered generator, it stretched immediately from bending to the PEDOT: PSS side to almost straight (Fig. 4b). This process is defined as the fast bending (FB) of the piezoelectric layer PVDF [38]. The water vapor was continuously applied after the final state of the PEDOT: PSS/PVDF double-layered generator that was reached. It maintained this state, which we define as the holding (HD) of the piezoelectric layer PVDF. When the PVDF was in the FB process, the piezoelectric output voltage rapidly increased to a maximum value, while the PVDF was in the HD process, the piezoelectric output voltage remained stable (Movie S3). During the HD process of the PVDF, water vapor was continuously applied. The water exchange between the PEDOT: PSS layer and the environment was a dynamic continuous process. Thus, the restraint of PEDOT: PSS layer on the PVDF layer and the effect of the force were dynamic, so that PVDF piezoelectric output voltage could maintain overall stability under the condition of small vibration. When stopped the application of water vapor, the PEDOT: PSS/PVDF double-layered generator gradually recovered from the nearly flat state to the initial state of bending towards PEDOT: PSS side (Fig. 4c). This process is defined as the slow releasing (SR) of the piezoelectric layer PVDF. When the PEDOT: PSS/PVDF double-layered generator had almost restored to the initial position and no more obvious displacement, there were still moisture exchanging between the PEDOT: PSS layer and the environment, which was a dynamic dehumidification process. As the internal moisture of the PEDOT: PSS layer and the environmental humidity reached equilibrium, the restraint of the PEDOT: PSS layer on the PVDF layer gradually restored stability. Therefore, when the PVDF was in the SR process, the piezoelectric output voltage exhibited a slow decrease (Movie S4). The relation between the piezoelectric output voltage produced by the PEDOT: PSS/PVDF double-layered generator under the condition of changing the ambient humidity and the time is shown in Fig. 4d and e. Fig. 4d corresponds with the FB and HD processes (Fig. 4b). The generator output voltage reached the maximum of 152 mV when the water vapor was applied for 3 s. With continuous application of water vapor, the voltage generally remained stable. Fig. 4e corresponds with the SR process (Fig. 4c). Stopped the application of water vapor, and then after a period of time, the output voltage had not dropped to 0. Select 200 s in the entire SR process, the voltage dropped 3 mV. The insets in Fig. 4d, e are enlarged view of the corresponding part of the curve, showing that the output voltage is oscillating in a small range, proving that the restraint and the force effect of the PEDOT: PSS layer on the PVDF layer are dynamic. As control, we did not apply water vapor to the PEDOT: PSS/PVDF double-layered generator, but rather pressed and stirred it, which made the output voltage an AC signal (Fig. S1, Fig. S2).

In order to prove that our PEDOT: PSS/PVDF double-layered generator is capable of supplying power; we designed a practical application circuit. The equivalent circuit diagram is shown in Fig. 4f. The light-emitting diode (LED) in the circuit needs 1.6 V to be lit up, while the maximum output voltage of our generator is 152 mV. Our solution is to connect the capacitors in series and charge the capacitors one by one using the generator, which is equivalent to add up each capacitor to reach the LED lighting voltage. When switched on, the LED was charged by the series

capacitors, and was instantly lit, as shown in Fig. 4f (Movie S5). The actual circuit picture is shown in Fig. S3.

#### 4. Conclusions

In conclusion, this investigation fabricated a PEDOT: PSS/PVDF double-layered actuator and generator with good moisture response in a simple and versatile method. PEDOT: PSS/PVDF strip exhibits excellent bidirectional bending properties and sensitive moisture response properties. The bending curvature of the PEDOT: PSS/PVDF strip changes from  $-191^\circ$  to  $225^\circ$  when RH is adjusted from 23% to 86%. Furthermore, a biomimetic dragonfly and a three-layer-structure flower are designed and fabricated, indicating that in the future the PEDOT: PSS/PVDF double-layered actuator can be used in the bionic, sensing, multi-level intelligent devices and other fields. The PEDOT: PSS/PVDF double-layered actuator is also a moisture-responsive generator. It converts the environmental humidity changes into mechanical displacement, and then converts the mechanical energy into electrical energy, achieving more than 150 mV stable DC voltage output. Finally, we designed a circuit to solve the problem that low-frequency small-signal DC voltage output is difficult to apply. It provides a new method for low-frequency small-signal energy collection and utilization, and provides a new strategy to solve the future energy problem.

#### Acknowledgments

This work was supported by the National Natural Science Foundation of China and National key research and development program under Grant #61435005, #61590930, #51335008, #51373064 and #2017YFB1104300.

#### Appendix A. Supplementary data

Supplementary data associated with this article can be found, in the online version, at <http://dx.doi.org/10.1016/j.snb.2017.08.125>.

#### References

- [1] C.F. Guo, T.Y. Sun, F. Cao, Q. Liu, Z.F. Ren, Metallic nanostructures for light trapping in energy-harvesting devices, *Light: Sci. Appl.* 3 (2014) e161.
- [2] H.L. Huang, Z. Yan, Present situation and future prospect of hydropower in China, *Renew. Sust. Energy Rev.* 13 (2009) 1652–1656.
- [3] F.D. Gonzalez, A. Sumper, O.G. Bellmunt, R.V. Robles, A review of energy storage technologies for wind power applications, *Renew. Sustainable Energy Rev.* 16 (2012) 2154–2171.
- [4] C.B. Field, J.E. Campbell, D.B. Lobell, Biomass energy: the scale of the potential resource, *Trends Ecol. Evol.* 23 (2008) 65–72.
- [5] P.D. Wright, Place attachment and public acceptance of renewable energy: a tidal energy case study, *J. Environ. Psychol.* 31 (2011) 336–343.
- [6] E. Barbier, Geothermal energy technology and current status: an overview, *Renew. Sustainable Energy Rev.* 6 (2002) 3–65.
- [7] F.X. Gao, W.W. Li, X.Q. Wang, X.D. Fang, M.M. Ma, A self-sustaining pyroelectric nanogenerator driven by water vapor, *Nano Energy* 22 (2016) 19–26.
- [8] L.D. Zhang, H.R. Liang, J. Jacob, P. Naumov, Photogated humidity-driven motility, *Nat. Commun.* 6 (2015) 7429.
- [9] M.M. Song, M.J. Cheng, M. Xiao, L.N. Zhang, G.N. Ju, F. Shi, Biomimicking of a swim bladder and its application as a mini-generator, *Adv. Mater.* (2017), 1603312.
- [10] M.M. Song, M. Xiao, L.N. Zhang, D.Q. Zhang, Y.T. Liu, F. Wang, F. Shi, Generating induced current through the diving-surfacing motion of a stimulus-responsive smart device, *Nano Energy* 20 (2016) 233–243.
- [11] M. Xiao, L. Wang, F.Q. Ji, F. Shi, Converting chemical energy to electricity through a three-jaw mini-generator driven by the decomposition of hydrogen peroxide, *ACS Appl. Mater. Interfaces* 8 (2016) 11403–11411.
- [12] X.H. Yu, J. Pan, J. Deng, J. Zhou, X.M. Sun, H.S. Peng, A novel photoelectric conversion yarn by integrating photomechanical actuation and the electrostatic effect, *Adv. Mater.* 28 (2016) 10744–10749.
- [13] L.N. Zhang, M.M. Song, M. Xiao, F. Shi, Diving-surfacing smart locomotion driven by a CO<sub>2</sub>-forming reaction, with applications to minigenerators, *Adv. Funct. Mater.* 26 (2016) 851–856.

- [14] M. Lee, C.Y. Chen, S.H. Wang, S.N. Cha, Y.J. Park, J.M. Kim, L.J. Chou, Z.L. Wang, A hybrid piezoelectric structure for wearable nanogenerators, *Adv. Mater.* 24 (2012) 1759–1764.
- [15] F.R. Fan, W. Tang, Z.L. Wang, Flexible nanogenerators for energy harvesting and self-powered electronics, *Adv. Mater.* 28 (2016) 4283–4305.
- [16] M.J. Villangca, D. Palima, A.R. Bañas, J. Glückstad, Light-driven micro-tool equipped with a syringe function, *Light Sci. Appl.* 5 (2016), e16148.
- [17] C. Lv, H. Xia, Q. Shi, G. Wang, Y.S. Wang, Q.D. Chen, Y.L. Zhang, L.Q. Liu, H.B. Sun, Sensitive humidity-driven actuator based on photopolymerizable PEG-DA films, *Adv. Mater. Interfaces* 4 (2017), 1601002.
- [18] G.C. Xu, J. Chen, M. Zhang, G.Q. Shi, An ultrasensitive moisture driven actuator based on small flakes of graphene oxide, *Sens. Actuators B* 242 (2017) 418–422.
- [19] E. Nawa, D. Yamamoto, A. Shioi, Chemotactic amoeboid-like shape change of a vesicle under a pH gradient, *Bull. Chem. Soc. Jpn.* 88 (2015) 1536–1544.
- [20] W. Zhang, H. Zappe, A. Seifert, Wafer-scale fabricated thermo-pneumatically tunable microlenses, *Light: Sci. Appl.* 3 (2014) e145.
- [21] Q. Zhao, J.W.C. Dunlop, X.L. Qiu, F.H. Huang, Z.B. Zhang, J. Heyda, J. Dzubielka, M. Antonietti, J.Y. Yuan, An instant multi-responsive porous polymer actuator driven by solvent molecule sorption, *Nat. Commun.* 5 (2014) 4293.
- [22] O. Sato, Dynamic molecular crystals with switchable physical properties, *Nat. Chem.* 8 (2016) 644–656.
- [23] K. Ariga, J.B. Li, J.B. Fei, Q.M. Ji, J.P. Hill, Nanoarchitectonics for dynamic functional materials from atomic-/molecular-level manipulation to macroscopic action, *Adv. Mater.* 28 (2016) 1251–1286.
- [24] K. Ariga, M. Naito, Q.M. Ji, D. Payra, Molecular cavity nanoarchitectonics for biomedical application and mechanical cavity manipulation, *CrystEngComm* 18 (2016) 4890–4899.
- [25] P. Fratzl, F.G. Barth, Biomaterial systems for mechanosensing and actuation, *Nature* 462 (2009) 442–448.
- [26] C. Dawson, J.F.V. Vincent, A.-M. Rocca, How pine cones open, *Nature* 390 (1997) 668.
- [27] J. He, P. Xiao, J.W. Zhang, Z.Z. Liu, W.Q. Wang, L.T. Qu, Q. Ouyang, X.F. Wang, Y.S. Chen, T. Chen, Highly efficient actuator of graphene/polydopamine uniform composite thin film driven by moisture gradients, *Adv. Mater. Interfaces* 3 (2016), 1600169.
- [28] D.D. Han, Y.L. Zhang, Y. Liu, Y.Q. Liu, H.B. Jiang, B. Han, X.Y. Fu, H. Ding, H.L. Xu, H.B. Sun, Bioinspired graphene actuators prepared by unilateral UV irradiation of graphene oxide papers, *Adv. Funct. Mater.* 25 (2015) 4548–4557.
- [29] I.H. Tseng, J.J. Li, P.Y. Chang, Mimosa pudica leaf-like rapid movement and actuation of organosoluble polyimide blending with sulfonated polyaniline, *Adv. Mater. Interfaces* (2017), 1600901.
- [30] M.M. Ma, L. Guo, D.G. Anderson, R. Langer, Bio-inspired polymer composite actuator and generator driven by water gradients, *Science* 339 (2013) 186–189.
- [31] L.D. Zhang, P. Naumov, Light- and humidity-induced motion of an acidochromic film, *Angew. Chem. Int. Ed.* 54 (2015) 8642–8647.
- [32] L.D. Zhang, S. Chizhik, Y.Z. Wen, P. Naumov, Directed motility of hydroresponsive biomimetic actuators, *Adv. Funct. Mater.* 6 (2016) 1040–1053.
- [33] S. Taccola, F. Greco, E. Sinibaldi, A. Mondini, B. Mazzolai, V. Mattoli, Toward a new generation of electrically controllable hygro-morphic soft actuators, *Adv. Mater.* 27 (2015) 1668–1675.
- [34] D.D. Han, Y.L. Zhang, H.B. Jiang, H. Xia, J. Feng, Q.D. Chen, H.L. Xu, H.B. Sun, Moisture-responsive graphene paper prepared by self-controlled photoreduction, *Adv. Mater.* 27 (2015) 332–338.
- [35] M. Wang, X.L. Tian, R.H.A. Ras, O. Ikkala, Sensitive humidity-driven reversible and bidirectional bending of nanocellulose thin films as bio-inspired actuation, *Adv. Mater. Interfaces* 2 (2015), 1500080.
- [36] M.C. Weng, P.D. Zhou, L.Z. Chen, L.L. Zhang, W. Zhang, Z.G. Huang, C.H. Liu, S.S. Fan, Multiresponsive bidirectional bending actuators fabricated by a pencil-on-paper method, *Adv. Funct. Mater.* 26 (2016) 7244–7253.
- [37] C. Chang, V.H. Tran, J.B. Wang, Y.K. Fuh, L.W. Lin, Direct-write piezoelectric polymeric nanogenerator with high energy conversion efficiency, *Nano Lett.* 10 (2010) 726–731.
- [38] D. Choi, K.Y. Lee, M.J. Jin, S.G. Ihn, S. Yun, X. Bulliard, W. Choi, S.Y. Lee, S.W. Kim, J.Y. Choi, J.M. Kim, Z.L. Wang, Control of naturally coupled piezoelectric and photovoltaic properties for multi-type energy scavengers, *Energy Environ. Sci.* 4 (2011) 4607–4613.

## Biographies

**Gong Wang** is currently a Master student at Jilin University, China. His research interests lie in the field of piezoelectric polymer, controlled deformations of soft actuators, energy device for energy conversion.

**Hong Xia** received her PhD degree in Chemistry from Jilin University, China, in 2006. She is currently a full professor at Jilin University. Her research interests include intelligent materials, stimulus-responsive actuators and laser microfabrication.

**Xiang-Chao Sun** is currently a Master student at Jilin University, China. His research interest has been focused on the technique of femtosecond laser direct writing to fabricate macro/nano devices.

**Chao Lv** is pursuing her Ph.D. at Jilin University, China. Her research interests include stimulus-responsive hydrogels and soft actuators.

**Shun-Xin Li** is pursuing her Ph.D. at Jilin University, China. Her research interests include organic crystal and nanofabrication.

**Bing Han** is pursuing her Ph.D. at Jilin University, China. Her research interests include bionic intelligent devices and new application of graphene.

**Qi Guo** is currently a Master student at Jilin University, China. His research interests lie in the field of circuit and system.

**Qing Shi** is currently a Master student at Jilin University, China. Her research interests include functional supramolecular hydrogels and stimulus-responsive actuators.

**Ying-Shuai Wang** is pursuing his Ph.D. at Jilin University, China. His research interests lie in the field of micro motor and application of nanocomposites.

**Hong-Bo Sun** received his Ph.D. in Electronic Science and Engineering from Jilin University in 1996. He is currently a full professor at Jilin University. His research interests have been focused on laser nanofabrication and ultrafast spectroscopy. He has published over 200 scientific papers in the above fields.